

Video Article

A Bioluminescent and Fluorescent Orthotopic Syngeneic Murine Model of Androgen-dependent and Castration-resistant Prostate Cancer

Jonathan F. Anker¹, Hanlin Mok¹, Anum F. Naseem¹, Praveen Thumbikat*^{1,3}, Sarki A. Abdulkadir*^{1,2,3}

¹Department of Urology, Northwestern University Feinberg School of Medicine

²The Robert H. Lurie Comprehensive Cancer Center, Northwestern University Feinberg School of Medicine

³Department of Pathology, Northwestern University Feinberg School of Medicine

*These authors contributed equally

Correspondence to: Praveen Thumbikat at thumbikat@northwestern.edu, Sarki A. Abdulkadir at Sarki.abdulkadir@northwestern.edu

URL: <https://www.jove.com/video/57301>

DOI: [doi:10.3791/57301](https://doi.org/10.3791/57301)

Keywords: Cancer Research, Issue 133, Prostate cancer, syngeneic mouse model, orthotopic prostate tumor, intra-prostatic injection, surgical castration, surgery, androgen-dependent prostate cancer, castration-resistant prostate cancer, urology, medicine, tumor microenvironment, *in vivo* imaging

Date Published: 3/6/2018

Citation: Anker, J.F., Mok, H., Naseem, A.F., Thumbikat, P., Abdulkadir, S.A. A Bioluminescent and Fluorescent Orthotopic Syngeneic Murine Model of Androgen-dependent and Castration-resistant Prostate Cancer. *J. Vis. Exp.* (133), e57301, doi:10.3791/57301 (2018).

Abstract

Orthotopic tumor modeling is a valuable tool for pre-clinical prostate cancer research, as it has multiple advantages over both subcutaneous and transgenic genetically engineered mouse models. Unlike subcutaneous tumors, orthotopic tumors contain more clinically accurate vasculature, tumor microenvironment, and responses to multiple therapies. In contrast to genetically engineered mouse models, orthotopic models can be performed with lower cost and in less time, involve the use of highly complex and heterogeneous mouse or human cancer cell lines, rather than single genetic alterations, and these cell lines can be genetically modified, such as to express imaging agents. Here, we present a protocol to surgically injecting a luciferase- and mCherry-expressing murine prostate cancer cell line into the anterior prostate lobe of mice. These mice developed orthotopic tumors that were non-invasively monitored *in vivo* and further analyzed for tumor volume, weight, mouse survival, and immune infiltration. Further, orthotopic tumor-bearing mice were surgically castrated, leading to immediate tumor regression and subsequent recurrence, representing castration-resistant prostate cancer. Although technical skill is required to carry out this procedure, this syngeneic orthotopic model of both androgen-dependent and castration-resistant prostate cancer is of great use to all investigators in the field.

Video Link

The video component of this article can be found at <https://www.jove.com/video/57301/>

Introduction

Prostate cancer is estimated to have the highest incidence (161,360 men) and cause the third-most male cancer deaths (84,590 men) in 2017¹. Upon diagnosis, prostate tumors are androgen-dependent, and are treated by surgical prostatectomy, radiation therapy, and/or androgen deprivation therapy (ADT), yet each treatment is associated with multiple major morbidities and complications^{2,3,4,5,6,7,8,9,10}. Despite tumor regression after ADT, nearly all tumors recur as castration-resistant prostate cancer (CRPC). At this stage, approved therapies include docetaxel, Sipuleucel-T immunotherapy, and the anti-androgen small molecules enzalutamide and abiraterone, yet no individual therapy confers a survival benefit of more than 5.2 months^{11,12,13,14,15,16,17}. Therefore, men at all stages of prostate cancer need both improved treatment options and management of morbidities, for which optimal pre-clinical disease modeling is crucial.

With correct procedure, prostate cancer cell lines can be surgically instilled into the murine prostate, leading to the development of both syngeneic or xenogeneic orthotopic tumors. Orthotopic tumor modeling is ideal for all tumor biology and drug development research, allowing for tumor development with a clinically representative tumor microenvironment (TME). Prior studies have demonstrated that subcutaneous (s.c.) tumors have an altered tumor vasculature, leading to differential and less clinically accurate responses to anti-angiogenic therapies^{18,19}. In addition, multiple studies have observed increased or decreased efficacy of multiple chemotherapeutics in treating the same cell line, depending on whether it was administered s.c. or orthotopically, the latter of which best represented what is seen in human cancer^{20,21,22}. Further, only in an orthotopic model of colon cancer, but not in the s.c. model, did tumors produce the correct degradative enzymes necessary to induce metastasis²³. Finally, as immunotherapies continue to emerge at the forefront of cancer therapy, and especially as they have yet to provide significant benefit for prostate cancer^{24,25}, syngeneic pre-clinical models with accurate TME and draining lymph nodes in immunocompetent hosts are critical.

There are many factors responsible for these inconsistent findings based on tumor site. With a different TME, cancer cells are exposed to different tissue-specific endothelium and altered angiogenesis, thereby affecting tumor development^{26,27}. Orthotopic tumors with the correct TME allow for clinically relevant drug delivery, hypoxic conditions, and evaluation of anti-angiogenic therapies²⁸. While genetically engineered models (GEMs) do contain an accurate TME, they require long times for breeding, high cost, and are often based on manipulations of single

or few genes knocked out or overexpressed beyond clinically relevant levels. In contrast, the human or murine prostate cancer cell lines used in orthotopic tumors, like human tumors, are much more genetically complex both within single cells and in displaying heterogeneity between cells^{29,30}. Also unlike GEMs, orthotopic cancer cell lines can be engineered to express imaging modalities or increased or decreased levels of other molecules of interest, and *in vitro* and *in vivo* experimental results can be directly compared. Orthotopic tumors can also be formed from primary patient-derived cells. Here, we report the methodology for performing intra-prostatic injections of prostate cancer cells that form orthotopic androgen-dependent tumors, and, after castration, recur as orthotopic CRPC.

Protocol

All of the animal procedures outlined in this protocol are to be performed in compliance with ethical regulations and the approval of the appropriate university Institutional Animal Care and Use Committee (IACUC).

1. Preparation of Surgical Materials and Cancer Cells

1. Before the day of surgery, autoclave the micro-dissecting scissors, Graefe forceps, Graefe tissue forceps, needle holder with suture cutters, and the appropriate number of drapes. Sterilize a 50 μ L syringe and 28-gauge needles by ethylene oxide gas (**Figure 1C**).
2. Before the day of surgery, culture Myc-CaP cells in 10 cm dishes in RPMI supplemented with 10% fetal bovine serum (FBS) and 1% penicillin/streptomycin (P/S) in a 37 °C 5% CO₂ incubator. For bioluminescent and/or fluorescent tumor monitoring, transfect 293T cells with the appropriate vectors and subsequently transduce Myc-CaP cells with 0.45 μ m filtered lentivirus³¹. Sort cells to generate a stable cell line with 100% transduction positivity.
NOTE: Perform all tissue culture under sterile conditions, and verify that all cell lines are mycoplasma-free. The murine prostate cancer cell line utilized in this study, Myc-CaP³², is transduced to stably express both firefly luciferase and mCherry. The Myc-CaP cell line is isolated from a *c-myc*-overexpressing Hi-myc mouse, and these cells contain an amplified androgen receptor (*AR*), which are androgen-dependent³² and form CRPC tumors after murine castration³³. All mice in this study are 6-8 week old male FVB/NJ mice. Alternative murine prostate cancer cell lines can be used with the mice of appropriate genetic background, as well as human prostate cancer cell lines or primary patient-derived prostate cancer cells with immunodeficient mice. The optimal number of cells per injection should be determined empirically for alternative cell lines. In addition, alternative imaging modalities can be utilized to visualize tumors, including magnetic resonance imaging (MRI), positron emission tomography (PET), or computed tomography (CT), as well as GFP as an alternative to mCherry.
3. The night before surgery, place matrigel basement membrane matrix and phenol red-free on ice at 4 °C to thaw.
4. On the day of surgery, collect the cells by washing them with phosphate buffered saline (PBS) and detaching with 0.25% trypsin-EDTA. Neutralize trypsin with RPMI with 10% FBS and 1% P/S.
5. Centrifuge the cells at 400 x g for 5 min.
6. Wash the cells with 10 mL of RPMI without FBS or P/S.
7. Count the cells and resuspend the cells in PBS at a concentration of 6.67x10⁷ cells/mL (1x10⁶ cells/15 μ L).
8. Add an equal volume of matrigel to create a 1:1 PBS/matrigel cell suspension at a final concentration of 1x10⁶ cells/30 μ L, and keep the cells on ice until injection to prevent solidification.
NOTE: Perform intra-prostatic injections within 3 h of preparing matrigel cell suspensions. If performing intra-prostatic injections on more than 5 mice, repeat the above steps to prepare a fresh matrigel cell suspension.

2. Pre-operative mouse preparation

NOTE: House mice in the university animal facility for at least one week before surgery to allow for adequate adaptation and to minimize animal stress. Steps 2.1-2.6 are performed by the surgeon assistant. All subsequent surgical steps are performed by the surgeon using sterile gloves and surgical tools with sterile technique.

1. Anesthetize the mice with isoflurane (2-5% for induction via chamber, 1-3% for maintenance via nose cone). Verify full induction by the loss of toe pinch reflex.
2. Weigh the mice and administer at least 0.05 mg/kg of the analgesic buprenorphine s.c.
NOTE: Mouse weight \geq 20 g is ideal for successful intra-prostatic injections.
3. Apply ophthalmic ointment lubrication to both eyes to prevent corneal drying.
4. Shave all fur from the abdomen.
5. Sterilize the abdomen by three rounds of circular application of surgical scrub using sterile non-adhering pads followed by sterile alcohol wipes. Allow the abdomen to dry.
NOTE: For the rest of the surgical procedure, only sterile gloves and surgical instruments can contact the sterilized mouse abdomen.
6. Transfer the mouse supine onto a clean surface on a heating pad directly under the objective of a clean surgical microscope.
7. Cover the mouse with a sterile drape with a small hole cut over the abdomen.

3. Intra-prostatic injection

NOTE: Perform all surgical steps under sterile conditions. Adjusting the microscope, the mouse placement, or any other non-sterile objects must be done by the surgeon assistant.

1. Perform an approximately 1 cm incision of the outer skin along the midline of the abdomen superior to the penis and the preputial glands (**Figure 1D**).
2. Separate the connective tissue between the outer abdominal skin and the inner abdominal musculature by opening the scissors between the layers.

3. Perform a similar incision of the inner abdominal musculature while using forceps to raise the musculature to avoid puncturing the intestines or bladder (**Figure 1D**).
4. Locate one of the bilateral seminal vesicles (**Figure 1A**, white)/anterior prostate lobes (**Figure 1A**, black), which are often posterior, lateral, and slightly superior to the bladder (**Figure 1A**, yellow), but this may vary between mice. The anterior prostate lobes are translucent and attached to the lesser curvature of the white seminal vesicles.
5. Gently raise the tip of the seminal vesicle using the Graefe tissue forceps to create tension on the tissue without puncturing the seminal vesicle (**Figure 1E**).
6. Mix the Myc-CaP matrigel solution by gentle pipetting (performed by the surgeon assistant), as cells may have pelleted, and slowly aspirate 30 μL (1×10^6 cells) into the needle to avoid air bubbles.
7. Carefully insert the bevel of the needle parallel to the long axis of the anterior prostate lobe. Slowly inject 30 μL into the lobe and slowly retract the needle to prevent leakage (**Figure 1F**). Verify adequate injection by engorgement of the anterior prostate lobe (**Figure 1G**).
8. Carefully hold the seminal vesicle and injected prostate lobe outside of the mouse for approximately 30 s to allow matrigel to partially solidify within the lobe. During this time, collect any cell solution leakage in the abdomen using a sterile polyester tipped applicator to prevent non-orthotopic tumor development, without pressing on the injected prostate lobe.
9. Carefully return the seminal vesicle and injected prostate lobe into the abdomen without putting pressure on the lobe. Replace any externalized tissues.
10. Perform continuous sutures to close the inner abdominal musculature with 5-0 vicryl absorbable reverse cutting needle sutures.
11. Perform interrupted sutures to close the outer abdominal skin with 4-0 nylon monofilament non-absorbable reverse cutting needle sutures. NOTE: Sterilized 9 mm staples can also be used to close the outer abdominal skin. However, in contrast to sutures, they interfere with any subsequent bioluminescent and fluorescent tumor imaging signal.
12. Clean all tools with sterile ethanol wipes (opened by the surgeon assistant) and place them in a glass bead sterilizer for 30 s. Allow the tools to dry before use on the next mouse.
13. Flush the syringe and needle in sterile saline (opened by the surgeon assistant) to prevent clogging by remnant matrigel. NOTE: A surgeon assistant should be present for all operations, performing all non-sterile pre-operative mouse preparation and post-operative mouse care, as well as to mix the Myc-CaP matrigel solution before injections. To minimize time, as each intra-prostatic mouse procedure will require 20-30 min, the surgeon assistant can begin preparing the next mouse as the surgeon is suturing the current mouse.

4. Post-operative Mouse Care

1. Administer 1 mg/kg of the analgesic meloxicam s.c. immediately, 24 h, and 48 h after surgery.
2. Allow mice to recover in a cage with no bedding placed halfway on a heating pad. Monitor mice for at least 30 min after surgery until they regain normal mobility and activity, after which place them in a clean cage with food on the floor of the cage.
3. Further monitor mice daily for proper wound healing, body weight, grooming, and ambulation after surgery. Separate mice into individual cages upon any evidence of fighting.
4. Remove any remaining sutures within 14 days after surgery.

5. Bioluminescent Tumor Imaging

1. Prepare sterile-filtered Na^+ or K^+ D-luciferin, as described by the manufacturer and protected from light.
2. Inject mice intra-peritoneally with 10 $\mu\text{L/g}$ of body weight of luciferin.
3. At least 10 min later, image mice with an IVIS Spectrum Imaging System, as previously described^{34,35}.
4. Analyze images using Living Image Software, as previously described^{34,35}. NOTE: IVIS imaging analysis is useful for determining successful intra-prostatic injections and initial tumor development to normalize tumor burden among experimental groups. However, depending on the intensity of the bioluminescent or fluorescent signal, saturation may cause a plateau in the image quantification despite an increase in actual tumor size. Therefore, in the later stages of tumor growth, IVIS imaging may be more useful to determine decreases in tumor size upon successful treatment rather than increases in size after image saturation.

6. Tumor Collection, Tumor Analysis, Survival Endpoint

1. If collecting tumor for analysis, humanely euthanize mice by CO_2 exposure and secondary cervical dislocation, or by alternative IACUC approved methods, and dissect tumors from the abdomen. Tumors should be located orthotopically at the prostate. NOTE: Tumors attached to the anterior abdominal wall or seeded throughout the abdomen indicate poor or leaky intra-prostatic injection, and should not be considered orthotopic tumors.
2. Weigh the tumors.
3. Calculate tumor volume as $\pi/6 \times L \times W \times H$ (L =length of the longest axis of the tumor, W =perpendicular width, H =perpendicular height).
4. Tumors can be analyzed by histology (fix in 10% neutral buffered formalin), flow cytometry (create single cell suspensions), protein (prepare tissue lysate in RIPA buffer), or RNA (immediately place tissue in RNA later).
5. For immunological analysis, also collect the prostate tumor-draining para-aortic lymph nodes (**Figure 1B**, orange) and the spleen. NOTE: If following mice for survival, the endpoint of this model is defined as the appearance of hemorrhagic abdominal ascites³⁶ and/or decreased ambulation, grooming, and/or piloerection³⁷. Mice for survival analysis receive pre- and post-operative analgesia (protocol steps 2.2, 4.1) and must be monitored regularly. Mice should be separated into individual cages if any fighting occurs, and should be humanely euthanized upon the appearance of any of the above endpoint readouts.

7. Surgical Castration to Model CRPC

1. To model CRPC, perform the above intra-prostatic injection protocol (protocol steps 1-5).
2. At least one week later, after tumor development, perform surgical castration via cauterization, as previously described³⁸.

3. Monitor tumor regression and recurrence by bioluminescent imaging. After castration, tumor regression will occur within 3 days and tumor recurrence will occur within approximately 30 days, representing CRPC.

Representative Results

In this manuscript, we surgically injected the murine prostate cancer cell line, Myc-CaP, into the anterior prostate lobe (**Figure 1A**), leading to the development of orthotopic prostate tumors with a clinically relevant TME and the correct prostate-draining lymph nodes (**Figure 1B**). This was performed using micro-dissecting scissors, Graefe forceps, Graefe tissue forceps, a needle holder with suture cutters, and a 50 μ L syringe with a 28-gauge needle (**Figure 1C**). After performing an approximately 1 cm midline abdominal incision above the preputial glands (**Figure 1D**), one seminal vesicle and attached anterior prostate lobe were located and externalized (**Figure 1E**) and 30 μ L (1×10^6 cells) of a 1:1 PBS/matrigel cell suspension was injected into the prostate (**Figure 1F**), as initially verified by the engorgement of the lobe and the lack of leakage (**Figure 1G**).

To monitor the orthotopic tumor growth, we stably transfected Myc-CaP cells to express both firefly luciferase and mCherry, allowing for tumors to be followed by non-invasive *in vivo* bioluminescence (**Figure 2A**) and fluorescence (**Figure 2B**), respectively. One limitation of this imaging is that, depending on the strength of the signal, imaging quantification may saturate while the tumor continues to increase in size. Therefore, with high signal intensities, this *in vivo* imaging is more useful for initially normalizing tumor burden across experimental groups and for later determining decreases in tumor size after experimental treatments. Additional imaging modalities can also be utilized, such as small animal MRI, PET, or CT.

Orthotopic tumors were dissected from the abdomen on day 30 after intra-prostatic injection (**Figure 3A**). Orthotopic tumors should be located at the site of the anterior prostate lobe. Tumor masses throughout the abdomen or attached to the anterior abdominal wall indicate improper intra-prostatic injection and leakage. With proper technique, tumor volume (**Figure 3B**) and weight (**Figure 3C**) can be recorded with relatively small standard error. However, as observed, there will be some variability with small and large tumor masses. Therefore, initial use of pre-treatment imaging quantification to equalize tumor burden between experimental arms is critical for all experiments. Further, as these murine cancer cells were injected into immunocompetent FVB/NJ mice, the TME can be analyzed by immunohistochemistry (IHC) (or flow cytometry or other techniques) for CD3 T cells (**Figure 3D**) (or other immune cell types). Finally, this model provides an objective survival endpoint, as the large primary tumor mass causes hemorrhagic abdominal ascites³⁶ (**Figure 3E**) and/or decreased ambulation, grooming, and/or piloerection³⁷. Occasionally, death may also be caused by tumor growth blocking urine output.

Finally, this model can be utilized to study both androgen-dependent prostate cancer and CRPC, the latter of which confers poor prognosis and is in need of novel treatment options. After orthotopic tumor development, mice were surgically castrated, as previously described³⁸. As this is the second major survival surgery, extra care must be given to monitor for recovery and any adverse events or complications. Within 3 days after castration, strong tumor regression was observed, followed by subsequent tumor recurrence after approximately 30 days, representing CRPC (**Figure 4A**). CRPC tumors can be dissection and analyzed histologically, and do not display any neuroendocrine differentiation, as they maintain high AR levels and are negative for the neuroendocrine marker, synaptophysin (**Figure 4B**).

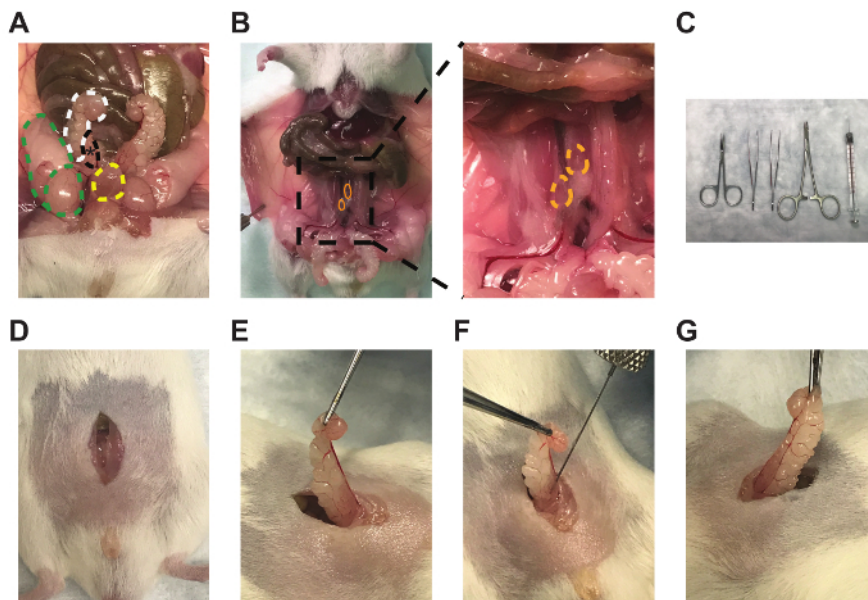


Figure 1: Anterior prostate lobe, draining lymph nodes, and representative technique for intra-prostatic cell injections. Images of the (A) right anterior prostate lobe (black, *), attached right seminal vesicle (white), right testicle and fat pad (green), and bladder (yellow), (B) bilateral prostate-draining para-aortic lymph nodes (orange), (C) micro-dissecting scissors, Graefe forceps, Graefe tissue forceps, an needle holder with suture cutters, and 50 μ L syringe with 28-gauge needle (left to right), (D) midline incisions, (E) seminal vesicle and anterior prostate lobe externalization, (F) intra-prostatic injection, and (G) engorgement of the anterior prostate lobe. [Please click here to view a larger version of this figure.](#)

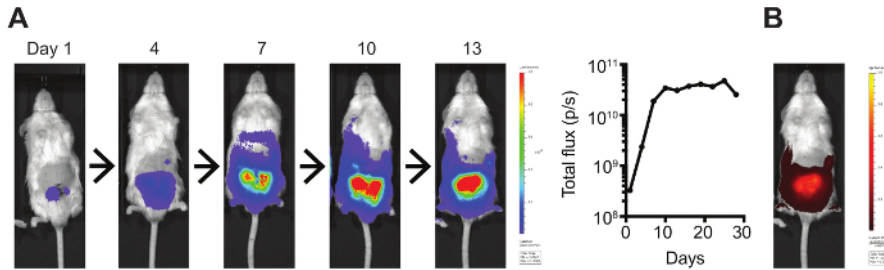


Figure 2: *In vivo* bioluminescent and fluorescent tumor imaging. (A) Luciferase- and (B) mCherry-expressing orthotopic Myc-CaP tumors were imaged using an IVIS Spectrum Imaging System. Bioluminescence was quantified by total flux (photons/s). [Please click here to view a larger version of this figure.](#)

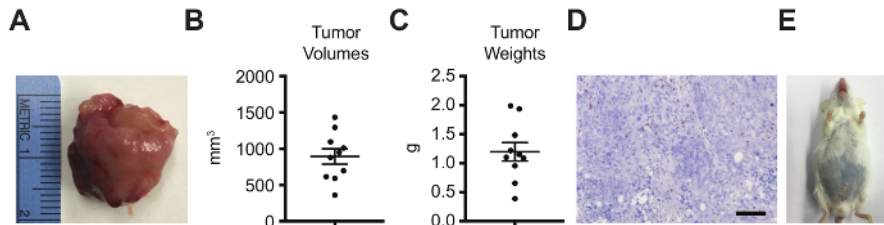


Figure 3: Orthotopic tumor analyses by tumor volume, weight, histology for immune infiltration, and survival. Orthotopic tumors were dissected on day 30 after intra-prostatic injection and analyzed by (A) gross imaging, (B) tumor volume ($\pi/6 \times L \times W \times H$; L=length of the longest axis of the tumor, W=perpendicular width, H=perpendicular height), (C) tumor weight, (D) CD3 IHC (scale bar=100 μ m), and (E) survival, with the objective endpoint as the appearance of hemorrhagic abdominal ascites. (A-B) Data represented as mean \pm standard error of the mean. [Please click here to view a larger version of this figure.](#)

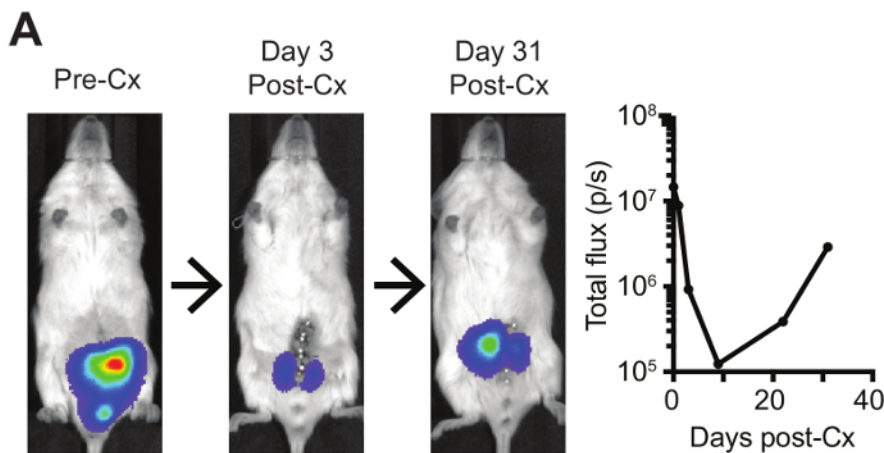


Figure 4: Intra-prostatic injections with subsequent surgical castration to model both androgen-dependent prostate cancer and CRPC. (A) Mice bearing orthotopic luciferase-expressing tumors were imaged by bioluminescence pre- and post-castration (Cx), and (B) recurred CRPC tumors were dissected (black=orthotopic prostate tumor; yellow=bladder) and analyzed by H&E, AR IHC, and synaptophysin IHC (with positive murine control) (scale bar=50 μ m). [Please click here to view a larger version of this figure.](#)

Discussion

In this manuscript we outline the protocol to perform surgical intra-prostatic cancer cell injections. We utilized the androgen-dependent and *MYC*-overexpressing (*MYC* overexpression is seen up to 80-90% of human prostate cancer³⁹) murine prostate cancer cell line, Myc-CaP, originally isolated from the Hi-Myc mouse^{32,33}. This cell line was stably transduced to express both luciferase and mCherry, for non-invasive *in vivo* bioluminescent and fluorescent tumor imaging, respectively. Further, surgical castration was also performed after androgen-dependent tumor development, leading to tumor regression and subsequent recurrence. Therefore, we provide details to model both orthotopic androgen-dependent prostate cancer and CRPC in an immunocompetent host.

Myc-CaP cells were injected into the anterior prostate lobe of mice. The mouse prostate consists of the anterior, ventral, and dorsolateral prostate lobes, and the human prostate consists of a peripheral zone, transitional zone, and central zone within a single lobe⁴⁰. While prior studies have anatomically and histologically compared the dorsolateral mouse lobe to the human peripheral zone, the site of the majority of prostate cancers⁴¹, and the anterior mouse lobe to the human central zone^{42,43}, more recent and comprehensive analysis has demonstrated that the anterior lobe and dorsolateral lobe display closely related gene expression patterns, as compared to the ventral lobe.⁴⁴ Further, prostate cancer development has been observed in the anterior lobe of GEMs⁴⁰, and, for the intra-prostatic procedure, the anterior lobe allows for the injection of the necessary volume of cancer cell solution with minimal leakage and variability.

Using s.c. and transgenic GEM cancer models have multiple flaws and limitations. S.c. tumors grown in an artificial TME have differential responses to chemotherapies, in contrast to both orthotopic tumors from the same cell lines and human disease^{20,21,22}. This may be due to the altered vasculature of s.c. tumors, as exemplified by their differential response to anti-angiogenic therapy^{18,19}. On the contrary, orthotopic tumors develop with a proper TME, draining lymph nodes, and vasculature, and can be performed with murine cell lines, thereby also allowing for analysis of tumor immunology and response to immunotherapies.

Transgenic GEMs develop tumors with a proper TME in an immunocompetent host, yet these models typically oversimplify human cancer by developing tumors with single or few genetic alterations²⁹. An analysis of Myc-CaP and other prostate cancer cell lines revealed that they contained much greater somatic copy number alterations and chromosomal alterations than tumors from the Hi-Myc mice and other GEMs from which they were derived²⁹. Further, GEMs are limited by the increased cost and time needed for mice breeding to perform experiments of sufficient power. Orthotopic tumor modeling can overcome these limitations. Human and murine prostate cancer cell lines contain many genetic alterations relevant to human disease²⁹, and, like human cancer, also show great heterogeneity between individual cells³⁰. Orthotopic murine syngeneic tumors allow for immunological analyses, while orthotopic human xenogeneic tumors allow for analyses of therapeutics on human cells. Finally, unlike with GEMs, cell lines can be modified before injection, allowing for expression of bioluminescent or fluorescent imaging molecules to monitor tumor growth, normalize tumor burden among experimental groups, monitor response to treatment, and to follow tumor regression and CRPC recurrence after surgical castration.

Critical steps in this protocol include locating and externalizing the seminal vesicle and attached anterior prostate lobe without damaging other tissues or puncturing the seminal vesicle, performing a successful intra-prostatic injection of the 30 μ L of cell suspension without leakage, and properly collecting any leakage to prevent non-orthotopic tumor development throughout the abdomen. The major limitation of intra-prostatic injections is attaining the technical skill required to minimize tumor variability between mice. This is especially important for modeling CRPC, which has the added variable of surgical castration. Intra-prostatically injected and castrated mice must also be followed closely for recovery and adverse events, as they have undergone two major survival surgeries. Another limitation is the time of each intra-prostatic injection. This can be reduced to as low as 20 min, and the surgeon assistant can prepare the next mouse as the current mouse is being sutured. Finally, orthotopic Myc-CaP tumors are aggressive, fast growing tumors that reach the survival endpoint in approximately 46 days (and as early as 35 days) due to the primary tumor mass. Studies requiring slower tumor development or long-term treatments should be optimized empirically for the initial injection cell count and treatment regimen. In contrast to the limitations of s.c. tumors and GEMs, all of the above limitations of the orthotopic tumor model can be overcome, and additional modifications of the protocol can be made based on individual experimental needs.

As the orthotopic tumor model involves the use of *in vitro*-handled cells, these cells can be modified depending on the needs of the study. Here, we modified these cells to stably express luciferase and mCherry for *in vivo* tumor monitoring. We have also performed a CRISPR-Cas9 knockout of the tumor suppressor *PTEN*, to generate a more aggressive, clinically relevant cell line that grows faster as orthotopic tumors (manuscript in review). With the advantages of the orthotopic tumor model, the ability to study both androgen-dependent prostate cancer and CRPC, and the potential to express imaging modalities or knockdown or overexpress select genes, this protocol serves as a valuable resource for all prostate cancer research.

Disclosures

The authors have nothing to disclose.

Acknowledgements

This work was supported by National Institutes of Health grants to Praveen Thumbikat (NIDDK R01 DK094898), Sarki Abdulkadir (NCI R01 CA167966, NCI R01 CA123484, NCI P50 CA180995), and Jonathan Anker (NCI F30 CA203472).

References

1. Siegel, R. L., Miller, K. D., & Jemal, A. Cancer Statistics, 2017. *CA-Cancer J Clin.* **67** (1), 7-30 (2017).
2. Alemozaffar, M. *et al.* Prediction of erectile function following treatment for prostate cancer. *JAMA.* **306** (11), 1205-1214 (2011).

3. Alibhai, S. M. *et al.* 30-day mortality and major complications after radical prostatectomy: influence of age and comorbidity. *J Natl Cancer I.* **97** (20), 1525-1532 (2005).
4. Chen, R. C., Clark, J. A., & Talcott, J. A. Individualizing quality-of-life outcomes reporting: how localized prostate cancer treatments affect patients with different levels of baseline urinary, bowel, and sexual function. *J Clin Oncol.* **27** (24), 3916-3922 (2009).
5. Kohutek, Z. A. *et al.* Long-Term Impact of Androgen-Deprivation Therapy on Cardiovascular Morbidity after Radiotherapy for Clinically Localized Prostate Cancer. *Urology.* (2015).
6. Murray, L. *et al.* Second primary cancers after radiation for prostate cancer: a systematic review of the clinical data and impact of treatment technique. *Radiother Oncol.* **110** (2), 213-228 (2014).
7. Resnick, M. J. *et al.* Long-term functional outcomes after treatment for localized prostate cancer. *N Engl J Med.* **368** (5), 436-445 (2013).
8. Shahinian, V. B., Kuo, Y. F., Freeman, J. L., & Goodwin, J. S. Risk of fracture after androgen deprivation for prostate cancer. *New Engl J Med.* **352** (2), 154-164 (2005).
9. Wilke, D. R. *et al.* Testosterone and erectile function recovery after radiotherapy and long-term androgen deprivation with luteinizing hormone-releasing hormone agonists. *BJU Int.* **97** (5), 963-968 (2006).
10. Zhao, J. *et al.* Androgen deprivation therapy for prostate cancer is associated with cardiovascular morbidity and mortality: a meta-analysis of population-based observational studies. *PLoS One.* **9** (9), e107516 (2014).
11. Berthold, D. R. *et al.* Docetaxel plus prednisone or mitoxantrone plus prednisone for advanced prostate cancer: updated survival in the TAX 327 study. *J Clin Oncol.* **26** (2), 242-245 (2008).
12. Bono, J. S. *et al.* Prednisone plus cabazitaxel or mitoxantrone for metastatic castration-resistant prostate cancer progressing after docetaxel treatment: a randomised open-label trial. *Lancet.* **376** (9747), 1147-1154 (2010).
13. Fizazi, K. *et al.* Abiraterone acetate for treatment of metastatic castration-resistant prostate cancer: final overall survival analysis of the COU-AA-301 randomised, double-blind, placebo-controlled phase 3 study. *Lancet Oncol.* **13** (10), 983-992 (2012).
14. Kantoff, P. W. *et al.* Sipuleucel-T immunotherapy for castration-resistant prostate cancer. *New Engl J Med.* **363** (5), 411-422 (2010).
15. Parker, C. *et al.* Alpha emitter radium-223 and survival in metastatic prostate cancer. *New Engl J Med.* **369** (3), 213-223 (2013).
16. Rathkopf, D. E. *et al.* Updated Interim Efficacy Analysis and Long-term Safety of Abiraterone Acetate in Metastatic Castration-resistant Prostate Cancer Patients Without Prior Chemotherapy (COU-AA-302). *Eur Urol.* **66** (5), 815-825 (2014).
17. Scher, H. I. *et al.* Increased survival with enzalutamide in prostate cancer after chemotherapy. *New Engl J Med.* **367** (13), 1187-1197 (2012).
18. Field, S. B. *et al.* Differences in vascular response between primary and transplanted tumours. *Brit J Cancer.* **63** (5), 723-726 (1991).
19. Cowen, S. E., Bibby, M. C., & Double, J. A. Characterisation of the vasculature within a murine adenocarcinoma growing in different sites to evaluate the potential of vascular therapies. *Acta Oncol.* **34** (3), 357-360 (1995).
20. Kuo, T. H. *et al.* Site-specific chemosensitivity of human small-cell lung carcinoma growing orthotopically compared to subcutaneously in SCID mice: the importance of orthotopic models to obtain relevant drug evaluation data. *Anticancer Res.* **13** (3), 627-630 (1993).
21. Fidler, I. J. *et al.* Modulation of tumor cell response to chemotherapy by the organ environment. *Cancer Meta Rev.* **13** (2), 209-222 (1994).
22. Wilmanns, C. *et al.* Modulation of Doxorubicin sensitivity and level of p-glycoprotein expression in human colon-carcinoma cells by ectopic and orthotopic environments in nude-mice. *Int J Oncol.* **3** (3), 413-422 (1993).
23. Fidler, I. J. Orthotopic implantation of human colon carcinomas into nude mice provides a valuable model for the biology and therapy of metastasis. *Cancer Meta Rev.* **10** (3), 229-243 (1991).
24. Kwon, E. D. *et al.* Ipilimumab versus placebo after radiotherapy in patients with metastatic castration-resistant prostate cancer that had progressed after docetaxel chemotherapy (CA184-043): a multicentre, randomised, double-blind, phase 3 trial. *Lancet Oncol.* **15** (7), 700-712 (2014).
25. Topalian, S. L. *et al.* Safety, activity, and immune correlates of anti-PD-1 antibody in cancer. *New Engl J Med.* **366** (26), 2443-2454 (2012).
26. Pasqualini, R., & Ruoslahti, E. Organ targeting in vivo using phage display peptide libraries. *Nature.* **380** (6572), 364-366 (1996).
27. Conway, E. M., & Carmeliet, P. The diversity of endothelial cells: a challenge for therapeutic angiogenesis. *Genome Biol.* **5** (2), 207 (2004).
28. Loi, M. *et al.* The use of the orthotopic model to validate antivascular therapies for cancer. *Int J Dev Biol.* **55** (4-5), 547-555 (2011).
29. Bianchi-Frias, D., Hernandez, S. A., Coleman, R., Wu, H., & Nelson, P. S. The landscape of somatic chromosomal copy number aberrations in GEM models of prostate carcinoma. *Mol Cancer Res.* **13** (2), 339-347 (2015).
30. Pan, Y. *et al.* Characterization of chromosomal abnormalities in prostate cancer cell lines by spectral karyotyping. *Cytogenet Cell Genet.* **87** (3-4), 225-232 (1999).
31. Wang, J. *et al.* Pim1 kinase synergizes with c-MYC to induce advanced prostate carcinoma. *Oncogene.* **29** (17), 2477-2487 (2010).
32. Watson, P. A. *et al.* Context-dependent hormone-refractory progression revealed through characterization of a novel murine prostate cancer cell line. *Cancer Res.* **65** (24), 11565-11571 (2005).
33. Ellis, L., Lehet, K., Ramakrishnan, S., Adelaiye, R., & Pili, R. Development of a castrate resistant transplant tumor model of prostate cancer. *Prostate.* **72** (6), 587-591 (2012).
34. Nunez-Cruz, S., Connolly, D. C., & Scholler, N. An orthotopic model of serous ovarian cancer in immunocompetent mice for in vivo tumor imaging and monitoring of tumor immune responses. *J Vis Exp.* (45) (2010).
35. Lim, E., Modi, K. D., & Kim, J. In vivo bioluminescent imaging of mammary tumors using IVIS spectrum. *J Vis Exp.* (26) (2009).
36. Ellis, L., Lehet, K., Ku, S., Azabdaftari, G., & Pili, R. Generation of a syngeneic orthotopic transplant model of prostate cancer metastasis. *Oncoscience.* **1** (10), 609-613 (2014).
37. Wallace, J. Humane endpoints and cancer research. *ILAR J.* **41** (2), 87-93 (2000).
38. Valkenburg, K. C., Amend, S. R., & Pienta, K. J. Murine Prostate Micro-dissection and Surgical Castration. *J Vis Exp.* (111) (2016).
39. Koh, C. M. *et al.* MYC and Prostate Cancer. *Genes Cancer.* **1** (6), 617-628 (2010).
40. Shappell, S. B. *et al.* Prostate pathology of genetically engineered mice: definitions and classification. The consensus report from the Bar Harbor meeting of the Mouse Models of Human Cancer Consortium Prostate Pathology Committee. *Cancer Res.* **64** (6), 2270-2305 (2004).
41. McNeal, J. E., Redwine, E. A., Freiha, F. S., & Stamey, T. A. Zonal distribution of prostatic adenocarcinoma. Correlation with histologic pattern and direction of spread. *Am J Surg Pathol.* **12** (12), 897-906 (1988).
42. Price, D. Comparative Aspects of Development and Structure in the Prostate. *Natl Cancer I Monogr.* **12** 1-27 (1963).
43. Roy-Burman, P., Wu, H., Powell, W. C., Hagenkord, J., & Cohen, M. B. Genetically defined mouse models that mimic natural aspects of human prostate cancer development. *Endocr-Relat Cancer.* **11** (2), 225-254 (2004).
44. Berquin, I. M., Min, Y., Wu, R., Wu, H., & Chen, Y. Q. Expression signature of the mouse prostate. *J Biol Chem.* **280** (43), 36442-36451 (2005).